Magnetoelectric direct and converse resonance effects in a flexible ferromagnetic-piezoelectric polymer structure

L.Y. Fetisov[a], D.V. Chashin[a], D.V. Saveliev[a], S.A. Afanasiev[a], I.D. Simonov-Emel'yanov[a], M.M. Vopson[b] and Y.K. Fetisov[a]

[a] MIREA - Russian Technological University, Moscow, Russia
[b] University of Portsmouth, Faculty of Technology, SMAP, Portsmouth, UK

Abstract

The direct and converse magnetoelectric (ME) effects in a flexible structure containing a mechanically coupled layers of amorphous ferromagnet FeBSiC and a piezo-polymer layer of polyviniledene-fluoride (PVDF) are investigated. The mutual transformation of magnetic and electric fields in the structure arises due to a combination of magnetostriction and piezoelectric effects in the ferromagnetic and piezoelectric layer, respectively. The ME effects were induced by exciting the structure with alternating magnetic fields of 0-100 kHz frequency and 1 – 5 Oe amplitude, or alternating electric fields of amplitudes up to 500 V/cm in the presence of a constant H field. For the direct ME effect the conversion coefficient reached 7.2 V/(cm·Oe) at a bending resonance frequency of 412 Hz and 44 V/(Oe·cm) at a planar resonance frequency of 25.15 kHz. Increasing the excitation magnetic field at the bending resonance frequency, the nonlinear second harmonic generation with an efficiency of 0.24 V/(Oe^{2}cm) was observed. For the converse ME effect, the conversion coefficient at the planar resonance frequency was 0.09 G·cm/V. The dependences of the efficiencies for the direct and converse ME transformations on the constant field and the amplitudes of the excitation fields are well explained by theory. These results could be used to develop magnetic and electric field sensors, as well as autonomous energy harvesting sources.

1. Introduction

The magnetoelectric (ME) effect exists in materials that simultaneously possess both the ferromagnetic and ferroelectric ordering and is manifested as an induced electric polarization of the sample in an external magnetic field (direct effect) or a change in the magnetization of the sample in an external electric field (converse effect) [1]. In composite structures containing alternating ferromagnetic (FM) and piezoelectric (PE) layers, the ME effects result from a combination of magnetostriction of the FM layer and piezoelectricity in the PE layer due to the mechanical coupling between the layers [2].

The magnitude of the direct effect is characterized by the ME coefficient $\alpha_E = \delta E / \delta H$, where δE is the amplitude of the generated electric field caused by a change in the magnetic field δH. The magnitude of the converse ME effect is characterized by the coefficient $\alpha_B = \delta B / \delta E$, where δB is the change in induction of the FM layer under the action of the electric field δE. In structures containing FM layers of materials with high magnetostriction λ (metals Ni, Co, alloys FeCo, FeGa, Terfenol-D, amorphous alloys, ferrites) and PE layers of materials with large piezo - modulus d (ceramics of lead zirconate titanate, lead magnesium niobate-lead titanate single crystals, AlN, langatate, quartz) the direct ME conversion coefficient can reach values α_E ~ 1-10 V/(cm·Oe), and converse ME coefficient α_B ~ 1 Gs·cm/V [3,4]. Both ~~the~~ effects are increased by ~2-3 orders of magnitude if the frequency of the excitation field coincides with the frequency of the acoustic resonance of the structure and the deformation in the structure increases resonantly [5].

Recently, much attention has been paid to the study of ME effects in structures with layers of amorphous ferromagnetic alloys FeBSiC and piezo-polymers (vinilidene fluoride-trifluoroethylene) (PVDF) [6-14]. The ferromagnetic alloys FeBSiC in the form of ribbons with a thickness of 20–30 μm are made by ultrafast cooling, they possess magnetostriction λ_S ~ (20-30)·10^{-6}, are saturated in weak magnetic fields H_S ~50 Oe, and are characterized by small magnetic and electrical losses [15]. The techniques for manufacturing 10-100 μm thick PVDF films, are also well developed. A piezo-polymer is characterized by a large ratio of piezo-modulus $d_{31} \approx$ 6-20 pC/N to the dielectric constant $\varepsilon \approx 12$, d_{31}/ε ~1, and low dielectric losses. These specific properties facilitate high efficiency of the ME transformation in the FeBSiC-PVDF structures. In

addition, such structures are flexible allowing their application on complex shape surfaces, and they are compatible with biological tissue, which is important for applications in medicine.

In the Metglas-PVDF structure, fabricated by gluing the layers, the ME coefficient of α_E = 7.2 V/(cm·Oe) over a wide frequency band and α_E~310 V/(cm·Oe) at a resonance frequency of 50 kHz was obtained [7]. In the monolithic structure made by deposition of the PVDF directly on the FeBSiC tape, the ME conversion coefficient α_E=850 V/(cm·Oe) in the resonant mode was achieved [12]. Based on the Metglas-PVDF structures, the magnetic fields sensors with sensitivity of 1.5 V/Oe [16], electric current sensors [17], magnetic memory elements [18], and autonomous energy sources [19] were proposed and fabricated.

Until now, only the direct dynamic ME effect was investigated in the Metglas-PVDF structures under alternating magnetic field excitations. The dependences of the direct ME conversion efficiency on the excitation field frequency, sample sizes [20], constant magnetic field [21], and temperature [22] were studied. The observation and studies of nonlinear effects of the frequency doubling and frequency mixing of magnetic fields were also reported [23].

The converse ME effect under excitation of the FeBSiC-PVDF structure by an alternating electric field has not been studied to date. In this article, we investigate both the direct and inverse ME effect in one FeBSiC-PVDF structure and we compare the effects with those observed in different structures. ~~It is the goal of this work.~~ The first part of the article describes the structure under investigation and measurement techniques. The second part contains the description of direct linear and nonlinear ME effects. In the third part, we describe, for the first time, the converse ME effect in the structure with PVDF piezo-polymer, followed by a detailed discussion of the results and conclusions on the work.

2. Sample and measurement setup

The structure under study is shown schematically in Fig. 1a, and its appearance in Fig. 1b. The FM layer was made of a tape of ~~an~~ amorphous FeBSiC alloy (Metglas 2605 SA1). It had the in-plane dimensions of 28 mm x 5 mm and a thickness of $a_m \approx 20$ μm. The PE layer was made of polyviniledene-fluoride piezo-polymer (PVDF) film. It had the in-plane dimensions of 28 mm x 5 mm and a thickness of a_p = 100 μm. Cu-electrodes ~ 0.5 μm thick were deposited on the surface of the PVDF layer by magnetron sputtering. After that, the PVDF layer was poled by heating up to 70°C, applying a constant electric field of 60 kV/cm for 30 minutes, and subsequent slow cooling in air.

The capacitance of the obtained capacitor was equal to c = 110 pF at a frequency of 100 Hz, which corresponds to the dielectric constant $\varepsilon \approx 10.4$. The PVDF piezoelectric modulus is d_{31} ≈10 pC/N. The ferromagnetic and PVDF layers were bonded under pressure using a fast drying epoxy adhesive. The structure was rigidly fixed at one end on a massive foundation, so that it could perform bending and planar oscillations. The length of the free part of the structure was L = 25 mm.

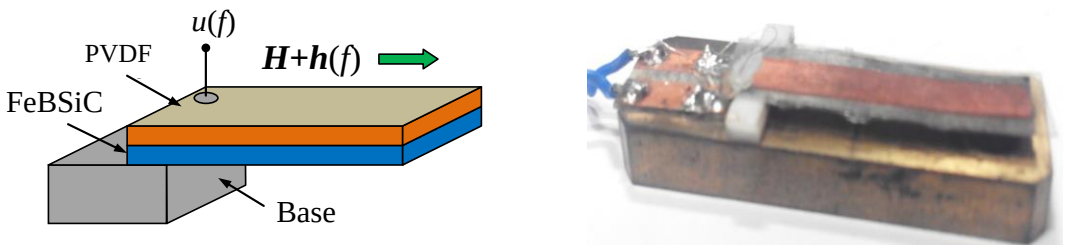

(a) (b)

Fig. 1 Schematic view (a) and appearance (b) of the FeBSiC-PVDF structure. Orientations of permanent H and excitation $h(f)$ magnetic fields are shown in (a).

Characteristics of the ME effects in the structure were studied using an automated installation described in [23]. The structure was placed in a constant magnetic field H = 0-100 Oe, created by the Helmholtz coils and directed tangentially along the long side of the structure. The field was measured with a LakeShore 421 Gaussmeter with an accuracy of 0.1 Oe. When studying the direct ME effect, the structure was placed inside an electromagnetic coil with a diameter of 60 mm. An ac current $I(f)$ from an Agilent 33210A generator was passed through the coil. The coil created the excitation magnetic field $h\cos(2\pi ft)$ with an amplitude h up to 6 Oe and frequency f = 10 Hz - 100 kHz. The voltage u generated by the PE layer of the structure was measured with an AKIP-2401 voltmeter. In the study of the converse ME effect, an electric voltage with an amplitude of up to 5 V and the same frequency from an Agilent 33210A oscillator was applied to the electrodes of the PVDF layer. This voltage created an excitation electric field with an amplitude of up to e =500 V/cm. The structure was placed inside an electromagnetic coil with a diameter of 20 mm, containing 500 turns of 0.2 mm in diameter wire. The coil converted the changes in the magnetic induction of the sample, caused by the converse ME effect, into an alternating output voltage. The frequency spectra of the generated voltage in both cases were recorded using a low-frequency SR770 FFT Network Analyzer. For both direct and converse ME effects, the dependences of the generated voltage u were measured as a function of the excitation frequency, the constant field H, the amplitudes of the excitation magnetic h and electric e fields.

3. Direct linear ME effect

Figure 2 shows the dependence of the voltage generated by the structure at the direct ME effect on the frequency of the excitation field f for H = 7 Oe. Two peaks are clearly visible: the low-frequency peak near the frequency f_1≈412 Hz with a height of u_1≈77 mV and quality factor of Q_1 ≈ 40 at 0.7 level, and high-frequency peak near the frequency of f_2 ≈25.15 kHz with amplitude of u_2≈177 mV and Q_2 ≈ 43. Far from the resonances, the voltage amplitude was ~2–4 mV. As will be shown shortly, a peak with frequency f_1 corresponds to the excitation of the lowest flexural vibration mode of the structure, while a peak with frequency f_2 corresponds to the excitation of the lowest planar oscillations mode along the length of the structure. The amplitude of the excitation field was h ≈1.1 Oe for the first peak and dropped to h ≈0.32 Oe for the second peak.

Figure. 3 shows measured dependences of the generated voltage on the constant magnetic field H for the low-frequency and high-frequency peaks. The data indicates that for both peaks the voltage first growths with increasing H, reaches the maximum at the same H_m ≈7.2 Oe, and then tends to zero at the saturation of the FM layer.

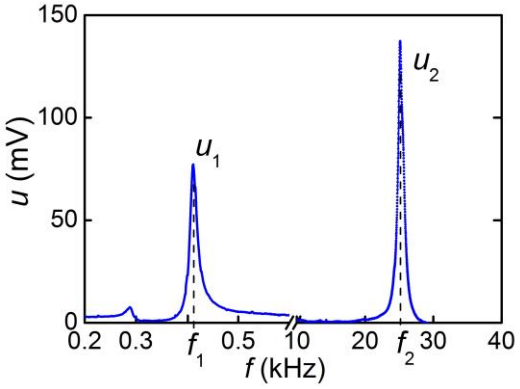

Fig. 2 Amplitude-frequency characteristics of the direct ME effect in the FeBSiC-PVDF structure at H ≈ 7 Oe.

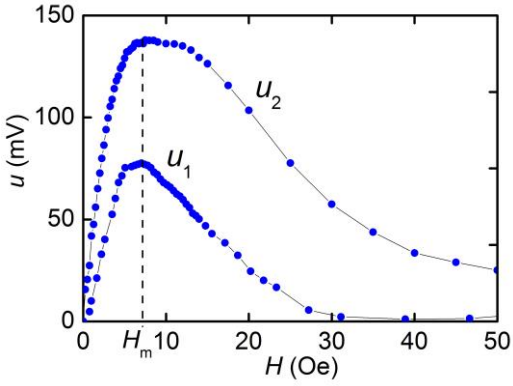

Fig. 3 Dependences of ME voltage vs. bias magnetic field H at direct ME effect for bending (u_1) and in-plane (u_2) resonances.

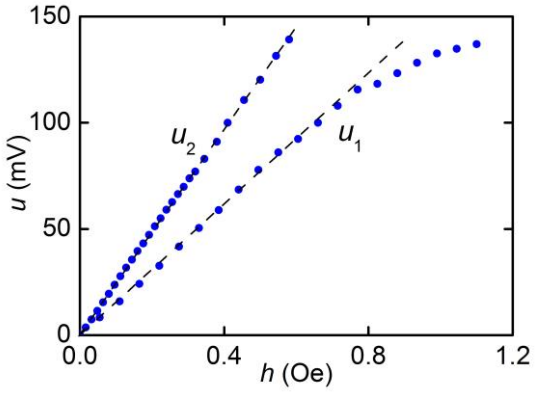

Fig. 4 Dependences of ME voltage for bending (u_1) and in-plane (u_2) resonances on the amplitude of excitation magnetic field h at direct ME effect.

Figure 4 shows the measured dependences of the height of resonant peaks shown in Fig. 2 on the excitation magnetic field amplitude h. The dashed lines depict the approximation of data by linear functions. The height of the low-frequency peak u_1 increases linearly with an increase in the excitation field up to h ~0.7 Oe, and then its growth rate slows. This indicates the nonlinear nature of the ME effect. At the same time, the height of the high-frequency peak u_2 increases linearly with an increase in the excitation field up to h ~0.6 Oe.

4. Direct nonlinear ME effect

Nonlinear phenomena were observed the direct ME effect when the excitation field h increases. As an example, Fig. 5 shows the frequency spectrum of ME voltage when the structure is excited by a harmonic magnetic field of fixed frequency f =206 Hz and amplitude h = 5.9 Oe without constant field, H = 0. The excitation frequency is set to half the frequency of the bending resonance of the structure. It is seen, that in addition to the direct electromagnetic leakage signal A_1 with the frequency of excitation field 206 Hz, ~~there are~~ second A_2 and fourth A_4 harmonics with frequencies $f_n = fn$ and amplitudes A_n, appeared in the spectrum, where n = 2, 4 .... The amplitudes of the harmonics monotonously decrease with increasing numbers.

Figure 6 shows the dependence of the 2nd harmonic amplitude A_2 on the constant field H. It is seen, that A_2 is maximum at H = 0, drops to zero in the field $H_m \approx 8$ Oe, then passes the local maximum and asymptotically tends to zero. In the next paragraph, we explain the form of the field dependence of the harmonic amplitude.

Figure 7 shows the dependence of the 2nd harmonic amplitude A_2 on the amplitude h of the excitation magnetic field. The dashed line depicts the approximation of the experimental data with a quadratic parabola. It is seen, that up to the fields h ~6 Oe, the amplitude of the second harmonic increases quadratically with increasing the field.

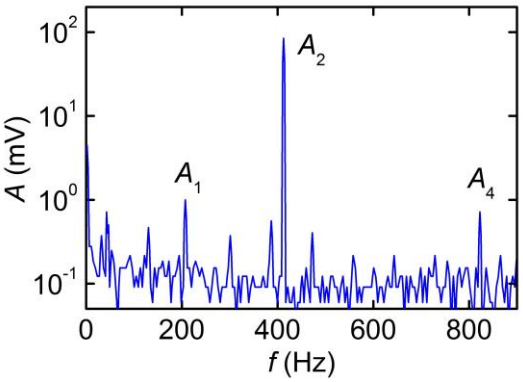

Fig. 5 Frequency spectrum of ME voltage under the structure excitation with harmonic magnetic field of frequency f=206 Гц and amplitude h= 5.9 Oe at H=0.

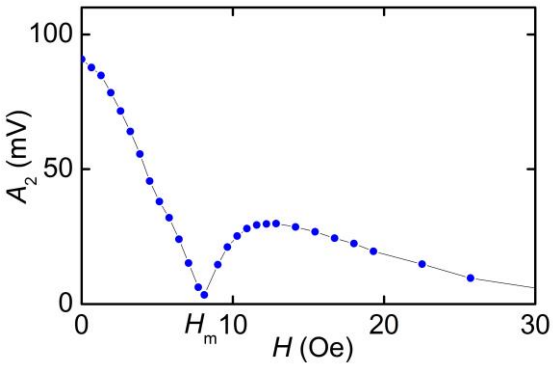

Fig. 6 Dependence of the 2-d voltage harmonics on constant bias field H at h=5.9 Oe at direct ME effct.

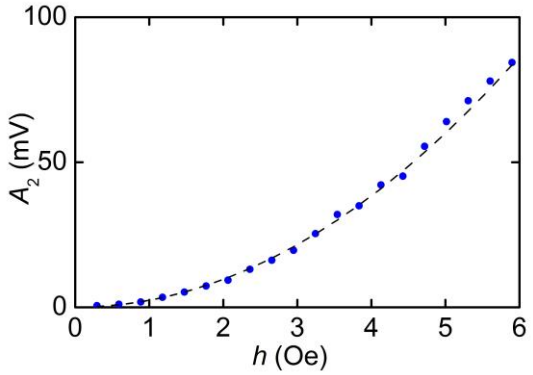

Fig. 7 Dependence of the 2-d harmonic amplitude A_2 on the amplitude of excitation field h for H=0 at direct ME effect.

When the structure was excited by alternating magnetic field with a frequency close to the resonance frequency of planar oscillations ~25 kHz, no nonlinear ME phenomena were observed. This is apparently due to the insufficient amplitude of the excitation field, which at the frequency of the planar resonance did not exceed 1.5 Oe.

4. Converse ME effect

Figure 8 shows the measured dependence of the voltage generated by the measuring coil for the converse ME effect as a function of the frequency of the excitation electric field, when its amplitude was set to e = 500 V/cm at H = 7.25 Oe. The peak near the frequency f_3 ≈25.5 kHz with an amplitude u_3 ≈ 38 mV and Q ≈ 53 at a level of 0.7 corresponds, as will be shown, to the excitation of the fundamental mode of longitudinal acoustic oscillations of the structure.

Figure 9 shows the dependence of the peak voltage at the converse ME effect on the constant field H. The voltage first increases linearly with increasing field, reaches a maximum at H_m ≈7.2 Oe, and then monotonously drops to zero at saturation of the FM layer. Note that the maximum conversion efficiency occurs approximately at the same magnetic field as for the direct effect (see Fig. 3).

Figure 10 demonstrates the dependence of the peak voltage, generated by the measuring coil, on the amplitude of the excitation electric field for H ≈ 7.2 Oe. The dashed line shows the approximation to a linear function, with a high level of agreement. ~~. It can be seen, that the dependence of a high linearity.~~ The relative standard deviation of the dependence on the linear law did not exceed 0.1%.

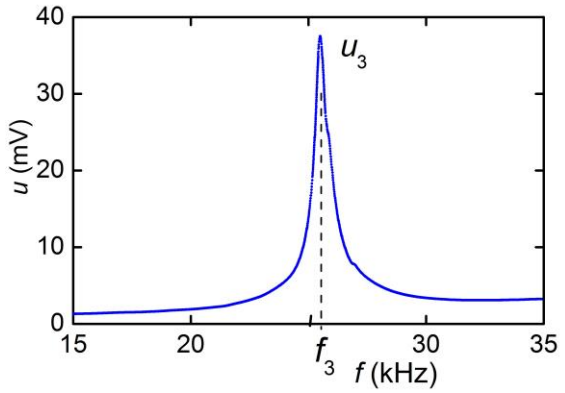

Fig.8 Amplitude-frequency characteristics of the converse ME effect in the FeBSiC structure at H=7.25 Oe and e = 500 V/cm.

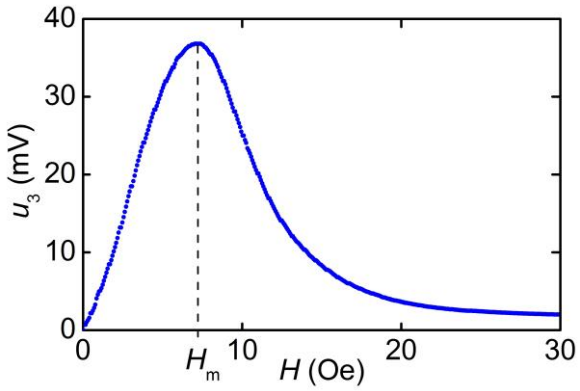

Fig. 9 Dependence of the generated voltage on bias magnetic field H at e= 500 V/cm for converse ME effect.

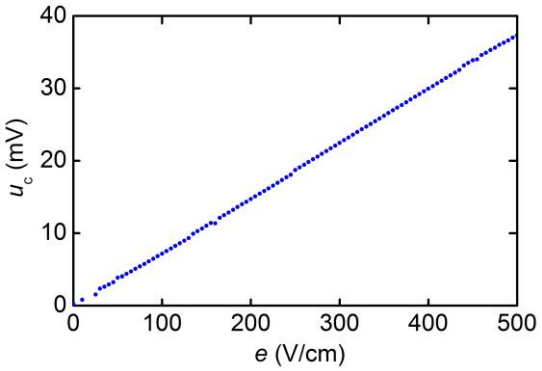

Fig. 10 Dependence of generated voltage on the amplitude of excitation electric field e at H=7 Oe for converse ME effect.

When the structure was excited with an electric field, the converse ME effect was absent at the resonance frequency of the flexural vibrations of the structure. Most likely, this is due to the use of the induction measurement method. The amplitude of the signal generated by the measuring coil is proportional to the frequency. At the frequency of bending resonance of the structure it was by a factor $f_1/f_2 \approx 60$ less than at the frequency of the planar resonance and was below the noise level. No nonlinear effects were observed when field amplitude increased up to e = 500 V/cm for the converse ME effect. This could be explained by the fact that the magnitude of the electric fields used was significantly smaller than the required repolarization field for the PVDF layer Ec ≈ 50 kV/cm, at which the deformation – electric field nonlinearity appears. The strains created by the piezo-polymer in the FeBSiC layer were also too small, which ensured the linear operation of the FM layer and the overall structure.

5. Discussion of the results

In order to explain the frequency dependences of the voltage $u(f)$ generated by the FeBSiC-PVDF structure at the direct and converse ME effects (see Fig. 2 and Fig. 8), let us estimate the frequencies of the acoustic resonances of the structure. The frequencies of bending f_1 and planar f_2 acoustic oscillations for a rectangular rod of length L, fixed at one end and free at the other end, are given by the formulas [24]:

$$f_1 = \frac{\beta_1}{2\pi}\frac{a}{L^2}\sqrt{\frac{Y}{12\rho(1-\gamma^2)}} \qquad \text{and} \qquad f_2 = \frac{1}{4L}\sqrt{\frac{Y}{\rho(1-\gamma^2)}}\,. \tag{1}$$

Here $\beta_1 = 22.4$ is the coefficient for the lowest mode of bending oscillations, Y is the Young's module, ρ is the specific density, and γ is the Poisson's coefficient. For the bilayer structure the effective values of the Young's module and specific density are given by the expressions:

$$Y = (Y_p a_p + Y_m a_m)/(a_p + a_m) \qquad \text{and} \qquad \rho = (\rho_p a_p + \rho_m a_m)/(a_p + a_m), \tag{2}$$

where $a = a_p + a_m$, a_p and a_m, ρ_p and ρ_m are the thicknesses and Young's moduli of the FM and PE layers (I guess you meant densities here?), respectively. Introducing in (2) the values of the layers' parameters [12] (PVDF: $Y_p = 9.5\cdot10^8$ N/m^2, $\rho_p = 2.7\cdot10^3$ kg/m^3; FeBSiC: $Y_m = 10.6\cdot10^{10}$ N/m^2, $\rho_m = 7.3\cdot10^3$ kg/m^3; γ≈0.35) and the dimensions of the layers, from (1) we find the frequency of the lowest mode of bending oscillations $f_1 \approx 432$ Hz and the frequency of the lowest mode of planar oscillations $f_2 \approx 23.6$ kHz. The obtained values are in good agreement with the measured ones. At these frequencies the efficiency of the ME conversion increases be a factor of Q ~ 40 due to the sharp increase in the mechanical deformations.

Note that resonance frequency for the direct ME effect f_2 = 25.15 kHz (Fig. 2) is slightly lower that the resonance frequency for the converse ME effect f_2 = 25.5 kHz (Figure 8). This is consistent with predictions of the theory that the maximum conversion for direct and converse effects occur at different frequencies [25,26], which differ slightly from each other.

Let us discuss the field dependences of the voltage $u(H)$ generated by the structure at direct (Fig. 3 and Fig. 6) and converse (Fig. 9) ME effects. For the direct ME effect, when the structure is excited by a harmonic magnetic field, the amplitudes of the voltage harmonics are given by the approximate expression [27]:

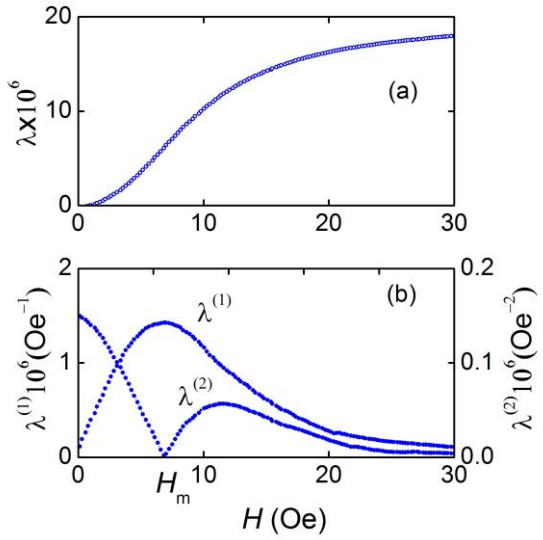

Fig. 11 Magnetostriction curve for the FeBSiC layer (a) and the 1-st and the 2-d derivatives of the magnetostriction over the field (b).

$$A_n \approx C_1 Q d_{31} \lambda^{(n)} h^n \qquad (3)$$

where n =1,2,3 .. is the harmonic number, C_1 is a constant coefficient depending only on the dimensions and mechanical parameters of the layers, Q is the acoustic resonance quality factor of the structure, d_{31} is the piezoelectric coefficient of the PE layer, $\lambda^{(n)} = \partial^n \lambda / \partial H^n \big|_{H=H_0}$ is the nth order derivative of the FM layer magnetostriction over the field, h is the amplitude of excitation magnetic field. It follows from (3), that field dependence of the amplitudes of the voltage harmonics $A_n(H)$ is determined by the shape of the field dependence of the corresponding derivative. The amplitude of the harmonics increases in a power-law manner with increasing excitation field h.

Figure 11(a) shows the dependence of the FeBSiC magnetostriction $\lambda(H)$ on the magnetic field, measured by strain gauge method [28]. Figure 11(b) shows the field dependences of the 1st and 2nd derivatives of the magnetostriction over the field, calculated by the numerical differentiation method using the data of Fig. 11(a). It is seen, that the curve $\lambda^{(1)}(H)$ qualitatively traces field dependences of the harmonics amplitude $u(H)$ (Fig. 3) for both bending and planar resonances. Maximum ~~of the~~ voltage at $H_m \sim 7$ Oe corresponds to the maximum of the 1st derivative. The field dependence of the 2nd derivative $\lambda^{(2)}(H)$ qualitatively repeats the field dependence of the second harmonic amplitude $A_2(H)$ in Fig.6. The derivative and voltage are both maximum at $H = 0$, fall to zero at the same magnetic field H_m, then pass the local maximum and again tend to zero. It follows from data in Fig. 7, that in accordance with the theory, the amplitude of the 2nd harmonic grows quadratically with increasing the amplitude h of the excitation field.

For the converse ME effect, when the structure is excited by an alternating electric field e, the amplitudes of the magnetic induction harmonics b_n are given by the expression [29]:

$$b_n \approx C_2 Q d_{31} b^{(n)} e^n \qquad (4)$$

where C_2 is the constant coefficient depending on the mechanical parameters and dimensions of the layers, $b^{(n)} = \partial^n b / \partial T^n \big|_{T=T_0}$ is the nth order derivative of the magnetic induction with respect to the stress, $b(T)$ is the dependence of the FM layer induction on the stress (elasto-magnetic effect), e is the amplitude of the excitation electric field. In [29], it was experimentally shown that the dependence of the coefficient $b^{(1)}$ on H has the shape similar to the dependence $u(H)$ shown in Fig. 9. The coefficient $b^{(1)}$ and the voltage u first linearly increase with increasing field, reach a maximum at $H_m \approx 7$ Oe, and then asymptotically tend to zero. The amplitude of the 1st voltage harmonic generated at the converse ME effect, as predicted by equation (4), increases linearly with increasing amplitude of excitation electric field e (see Fig. 10).

Now, let us estimate transformation coefficients for the linear and nonlinear direct and converse ME effects.

The coefficient of the direct ME effect at a bending resonance frequency is $\alpha_E \approx 7.2$ V/(Oe·cm), and at a planar resonance frequency is $\alpha_E \approx 44$ V/(Oe·cm). The obtained coefficients are an order of magnitude higher than for a similar structure with thin PVDF layer [23] and are comparable with coefficients for the structures made of other materials [3,4]. The efficiency of the second harmonic generation at the direct ME effect was 0.24 V/(Oe^{2}cm), which is higher by

a factor of ~10 than the efficiency of the second harmonic generation in the structure with thin PVDF layer [23] and is comparable to the efficiency for the Ni- PZT structure [26].

A specific feature of the structure under consideration is the significant difference in the mechanical rigidity of the layers: the Young's modulus of the FeBSiC layer is ~2 orders of magnitude larger than the Young's modulus of the PVDF layer. It was shown in [33] (formula 16), that maximum value of the ME coefficient in two-layer structures is achieved for the ratio of the layers thickness $a_p / a_m \approx \sqrt{Y_p /(Y_m \beta)}$, where $\beta \approx 1$ is the coefficient of mechanical coupling between the layers. Substituting the structure parameters into the formula, we obtain the optimal thickness of the PVDF layer $a_p \approx 10.5 \cdot a_m \approx 210$ μm. It follows that relatively "thick" PVDF films should be used to increase the efficiency of ME transformations in composite structures with Metglas layers.

In order to estimate the coefficient of the converse ME transformation, we first determine the change of the magnetic induction in the structure, by using the law of electromagnetic induction $A = N \cdot \delta B \cdot S \cdot 2\pi f_1$. Here, A is the amplitude of the harmonic generated by the measuring coil. For area S, we take the cross section of the FM film of 0.1mm^2, since the induction of the field varies only within the FM layer. For parameters corresponding to the data in Fig. 8 and e = 500 V/cm, we obtain $\delta B \approx 47$ G. Then, the coefficient of the converse ME transformation is 0.09 G·cm/V. The obtained coefficient is comparable to the conversion coefficient ~0.12 G·cm/V for the FeGa-PZT structure [31], ~0.055 G·cm/V for the Terfenol-PZT structure [32], and approximately two times smaller than the conversion coefficient for the Ni -PZT structure ~0.27 G·cm/V [33].

The results show the promising use of FeBSiC-PVDF structures for creating multifunctional sensors of magnetic and electric fields. The linear dependence of the ME voltage on the magnetic field (Fig. 3) in the range from zero to ~2 Oe and the high harmonic generation efficiency at the direct ME effect can be used to create a sensor of constant magnetic fields similar to that described in [34]. The linear dependence of the output signal on the electric field (Fig. 10) at the converse ME effect in combination with high sensitivity could be used to create non-contact sensors of low-frequency electric fields [35].

6. Conclusion

Thus, the direct and converse ME effects in a flexible structure containing an amorphous ferromagnetic FeBSiC layer and a piezo-polymer PVDF layer are experimentally investigated. In the case of the direct ME effect with the composite under excitation by an alternating magnetic fields, the nonlinear harmonic generation was clearly observed, arising due to the nonlinear dependence of the ferromagnetic layer magnetostriction on the magnetic field. When the structure was excited by alternating electric fields, the converse ME effect was observed due to the nonlinearity of the elastomagnetic properties of the ferromagnetic layer. The efficiency of mutual linear and nonlinear transformation of alternating magnetic and electric fields in the FeBSiC-PVDF structure is comparable with the efficiency of the fields' conversion in magnetoelectric structures of other materials**.**

Acknowledgments

The research was supported by the Ministry of Education and Science of Russia (project 8.1183.2017) and the Russian Foundation for Basic Research (grant 16-32-50095-mol).

References

1. L.D. Landau, E.M. Lifshitz, Elektrodinamika sploshnykh sred (Electrodynamics of coutinuous Media), Moscow: Nauka, 1982.
2. J. Van Suchtelen, Product properties: A new application of composite materials. Philips Res. Rep. 27 (1972) 28.
3. C.-W. Nan, M.I. Bichurin, S. Dong, Multiferroic magnetoelectric composites: Historical perspective, status, and future directions, JAP, 103 (2008). 031101.
4. M.M. Vopson, Fundamentals of Multiferroic Meterials and Their Possible applications, Cruitical Reviews in Solid State and Material Sciences, 0 (2014) 1-28.
5. M.I. Bichurin, D.A. Filippov, V.M. Petrov, V.M. Laletin, N. Paddubnaya, G. Srinivasan, Resonance magnetoelectric effects in layered magnetostrictive-piezoelectric composites, Phys. rev. B, 68 (2003) 132408
6. N. Cai, J. Zhai, L. Liu, Y. Lin, C.-W. Nan, The magnetoelectric properties of lead zirconate titanate/terfenol-D/PVDF laminate composited, Mater. Science and Eng.,B99 (2003) 211.
7. J Xing, J. Zhai, S. Dong, Z.. Li, and D. Viehland Giant magnetoelectric effect in Metglas/polyvinylidene-fluoride laminates // Appl. Phys. Let. – 2006. V. 89. № 083507.
8. Z. Fang, S.G. Lu, F. Li, S. Datta, Q.M. Zhang, M.E. Tahchi, Enhancing the magnetoelectric response of metglas/polyvinylidene fluoride laminates by exploiting the flux concentration effect // Appl. Phys. Lett. – 2009. V 95. P. 1–3.
9. S.G. Lu, J.Z. Jin, X. Zhou, Z. Fzng, Q. Wang, Q.M. Zhang, Large magnetoelectric coupling coefficient in poly(vinilidene fluoride-hexafluoropropylene)/Metglas laminates, J. Appl. Phys. 110 (2011) 104103.
10. P. Martins, S. Lanceros-Méndez, Polymer-Based Magnetoelectric Materials, Adv. Funct. Mater. 23 (2013) 3371.
11. M. Silva, S. Reis, C.S. Lehmann, P. Martins, S. Lanceros-Mendes, A. Lasheras, J. Gutierrez, J.M. Barandiran, Optimization of the magnetoelectric responce of poly(vinylidene fluoride)/epoxy/Vitrovac Laminates, Appl. Mater. Interfaces, 5 (2013) 10912.
12. A. Kulkarni, K. Meurisch, I. Teliban, R. Jahns, T. Strunskus, A. Piorra, R. Knochel, and E. Faupel, Giant magnetoelectric effect at low frequencies in polymer based thin film composites, APL, 104 (2014) 022904.
13. M. P. Silva, P. Martins, A. Lasheras, J. Gutiérrez, J. M. Barandiarán, S. Lanceros-Mendez Size effects on the magnetoelectric response on PVDF/Vitrovac 4040 laminate composites // JMMM. 2015. V. 377. P. 29–33.
14. Y.Long, J. Qiu, X.He, Q. Chang, Z. Hu, H. Liu. Flexible magnetoelectric transducer with high magnetic field sensitivitybased on Metglas/poly(vinylldene fluoride) heterostructures, AIP Advances 7 (2017) 124029.
15. https://metglas.com/magnetic-materials/
16. S.Reis, N. Caetro, M.P. Silva, V. Correira, J.G. Rocha, P. Martins, S. Lanseros-Mendes, Fabrication and characterization of high-performance polymer-based magnetoelectric DC magnetic field sensors devices, IEEE Trans on Industr. Electr., 64 (2017) 4828-4934.
17. M-Q Le, F. Behora, A. Comogolub, P.-J. Cottinet, L. Lebrun, A. Hajjaji, Enhenced magnetoelectric effect for flexible current sensor applications, J. Appl. Phys., 115 (2014) 194103.
18. P. Lu, D. Shang, J. Shen, Y. Chai, C. Yang, K. Zhai, J. Cong, S. Shen, Y. Sun, Nonvolatile transtance change random access memory based on magnetoelectric P(VDF-TiEF)/Metglas heterostructures, Appl. Phys. Lett.. 109 (2016) 252902.
19. A. lasheras, J. Gutierres, S. Reis, D. Sousa, M. Silva, P. Martins, S. Lanseros-Mendez, J.M. Barandiaran, D.A. Shishkin, A.P.Potapov, Energy harvesting devices based on metallic glases/PVDF magnetoelectric laminated composite, Smart. Mater. Struc. 24 (2015) 065024.

20. A. Lasheras, J. Gutierrez, J.M. Barandiaran, Quantification of size effects in the magnetoelectric response of metallic galss/PVDF laminates, Appl. Phys. Lett., 108 (2016) 222903.
21. J. Li, Y. Li, D. Zhu, Q. Wang, Y. Zhang, Y. Zhu, M. Li, Magnetoelectric effect modulation in a PVDF/Metglas/PVDF composite by applying DC electric fields on the PZT phase, J. Alloys and Comp., 661 (2016) 38-42.
22. J. Gutierrez, A. Lasheras, J.M. Barandiaran, J.L. Vilas, M.S. Sebastian, L.M. Leon, Temperature response of magnetostrictive/piezoelectric polymer magnetoelectric laminates, Key Engineering Materials, 495 (2012) 351.
23. L.Y. Fetisov, I.A. Baraban, Y.K. Fetisov, D.A. Burdin, M.M. Vopson, Nonlinear magnetoelectric effects in flexible composite ferromagnetic-piezopolymer structures, J. Mag. Magn. Mater., 441 (2017) 628-634.
24. Timoshenko S. (1961), *Vibration Problems in Engineering*, New York: D. Van Nostrand, p. 307
25. D.A. Filippov, V.M. Laletin, G. Srinivasan, Low-frequency and resonance magnetoelectric effects in nickel ferrite - PZT bulk composites, Technical Physics, 57 (2012) 44-47.
26. G. Wu, T. Nian, R. Zhang, N. Zhang, S. Li, N.X. Sun, Inequivalence of direct and converse magnetoelectric coupling at electromechanical resonance, Appl. Phys. Lett., 103 (2013) 182905.
27. D.A. Burdin, D.V. Chashin, N.A. Ekonomov, L.Y. Fetisov, Y.K. Fetisov, G. Sreenivasulu, G. Srinivasan, Nnolinear magnetoelectric effects in ferromagnetic-piezoelectric composites, J. Magn. Mag. Mater., **358** (2014) 98-104.
28. D.V. Chashin, D.A. Burdin, L.Y. Fetisov, N.A. Ekonomov, Y.K. Fetisov, Presize measurements of magnetostriction of ferromagnetic plates, J. of Siberian Federal Univ. Math. and Phys., 11 (2018) 30-34.
29. L.Y. Fetisov, D.V. Chashin, D.A. Burdin, D.V. Saveliev, N.A. Ekonomov, G. Srinivasan, Y.K. Fetisov, Nonlinear converse magnetoelectric effects in a ferromagnetic-piezoelectric bilayer, Appl. Phys. Lett., 113 (2018) 212903.
30. D.A. Filippov, Theory of the magnetoelectric effect in ferromagnetic-piezoelectric heterostructures, Phys. Solid State, 47 (2005) 1118-1121.
31. Y.K. Fetisov, K.E. Kamentsev, D.V. Chashin, L.Y. Fetisov, G. Srinivasan, Converse magnetoelectric effects in a galfenol and lead zirconate titanate bilayer, J. Appl. Phys., 105 (2009) 123918.
32. P. Record, C. Popov, J. Fletcher, E. Abraham, Z. Huang, H. Chang, R.W. Whatmore, Direct and converse magnetoelectric effect in laminate Terefenol-D-PZT composites, Sensors and Actuators B: Chemical, 126 (2007) 344-349.
33. Y.K. Fetisov, V.M. Petrov, G. Srinivasan, Inverse magnetoelectric effects in a ferromagnetic-piezoelectric layered structures, J. of Mater. Res. 22 (2007) 2074-2080.
34. V.N. Serov, L.Y. Fetisov, Y.K. Fetisov, E.I. Shestakov, High sensitivity magnetometer based on magnetoelectric sensor, Russian Technological J., 4 (2016) 24-37.
35. F. Xue, J.Hu, S.X. Wang, J. \He, In-plane longitudinal converse magnetoelectric effect in laminated composites: Aiming at sensing wide range electric field, Appl. Phys. Lett., 106 (2015) 082901.